

Beam experiments with Crab Cavities in KEKB

R. Tomás,* Y. Sun, and F. Zimmermann
CERN, CH 1211 Geneva 23, Switzerland

Y. Funakoshi, T. Ieiri, Y. Morita, K. Nakanishi, K. Ohmi, K. Oide, Y. Onishi, and M. Tobiyama
KEK, Tsukuba, Ibaraki 305-0801, Japan

R. Calaga
BNL, Upton, NY 11973, USA
(Dated: August 5, 2010)

During 2008 and 2009 dedicated beam experiments with crab cavities were performed in KEKB with two goals. The first goal was to measure the impact of crab cavity Radio Frequency (RF) noise in the beam quality. The second goal was to test procedures for the measurement of the crab dispersion. These experiments were performed as a validation of the crab cavity beam dynamics models in view of the possible use of crab cavities in the upgrade of the CERN Large Hadron Collider (LHC). The measurements are presented in this paper together with model predictions.

PACS numbers: 41.85.-p, 29.20.dk, 29.27.Eg

I. INTRODUCTION

The KEKB is an asymmetric electron-positron collider. The accelerator consists of a 3.5 GeV positron storage ring (LER) and an 8 GeV electron ring (HER) [1]. The KEKB electron and positron bunches cross at a 22 mrad angle in the Belle detector. KEKB has achieved world record luminosities in 2009 after the installation of one crab cavity per ring in 2007. These cavities give a time dependent transverse deflection to the beams that results in head-on collisions at the interaction point (IP).

The LHC upgrade could incorporate crab cavities in order to maximize the luminosity gain [2]. However, unlike the KEKB, the LHC features a negligible synchrotron radiation damping. This calls for the use of accurate models of crab cavity beam dynamics in order to validate an LHC upgrade based on crab cavities. Beam experiments were conducted in KEKB in order to study two critical aspects, the impact of crab cavity RF noise in the beam

quality and techniques to measure crab dispersion. Table I shows the machine parameters during the December 2008 crab cavity experiments in KEKB.

II. CRAB CAVITY RF PHASE NOISE

For several years crab cavity RF phase noise has been a concern [3] since it results in off-center collisions at the IP. In the absence of radiation damping even small phase errors could cause a time-cumulative emittance blow-up. In lepton machines, however, the excitation due to the phase error should reach a steady state thanks to the synchrotron radiation (at least for a small enough phase noise).

The phase noise of the KEKB crab cavities is dominated by a set of discrete frequencies [2]. Therefore it is justified to study the effect of phase noise at well defined frequencies, rather than to assume white noise.

During the beam experiments a sinusoidal phase modulation was fed into the KEKB crab cavities while beams were in collision. The usual transverse feedback against multibunch instabilities [4, 5] was switched on. Amplitude scans of the input noise were performed for two modulation frequencies close to the horizontal and vertical tunes, respectively. Luminosity was recorded during these scans. Figures 1 and 2 show the luminosity versus noise amplitude of the HER and LER crab cavities, respectively. The frequency of the sinusoidal noise in these two cases is set close to the horizontal tune of the machine. Results from simulations including the beam-beam interaction, the feedback system and the sinusoidal noise are compared to the measurements showing an excellent agreement. The most striking feature observed both in measurements and simulations is the existence of a threshold in the noise amplitude for the development of an instability causing the abrupt drop of luminosity. This threshold happens at an IP equivalent beam motion

TABLE I: Machine parameters during the December 2008 crab cavity experiments in KEKB.

	Unit	HER	LER
Particle		e ⁻	e ⁺
Particles per bunch	10 ¹⁰	4.1	6.3
Number of bunches		100	100
Horizontal emittance (ϵ_x)	nm	24	18
Horizontal tune (Q_x)		44.522	45.524
Vertical tune (Q_y)		41.602	43.585
Synchrotron tune (Q_s)		0.021	0.025
Revolution frequency	kHz	99.4	99.4
Damping time	ms	23	23

*Electronic address: rogelio.tomas@cern.ch

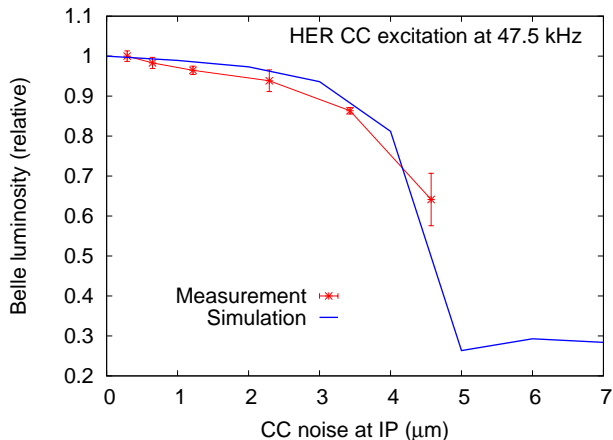


FIG. 1: Luminosity versus HER crab cavity noise as extrapolated to IP displacement. The noise frequency is close to the HER horizontal tune.

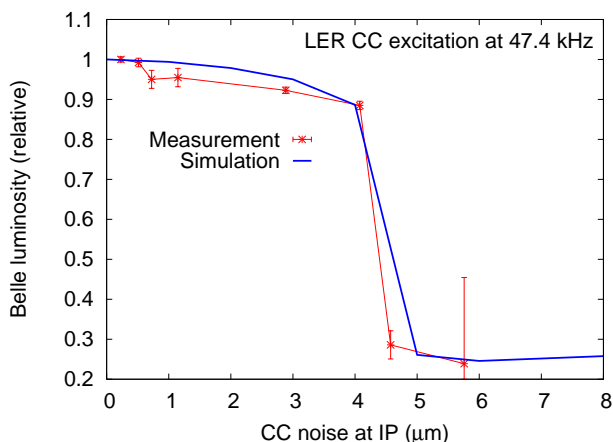


FIG. 2: Luminosity versus LER crab cavity noise as extrapolated to IP displacement. The noise frequency is close to the LER horizontal tune.

of about $4.5 \mu\text{m}$ ($\approx 0.015\sigma_x^*$ or ≈ 0.2 degrees for the LER case). To compute the IP equivalent beam motion from the CC phase noise the following equation is used,

$$x_{noise} \approx \frac{c}{\omega} \tan\left(\frac{\theta}{2}\right) \phi_{noise} \quad (1)$$

where $\theta/2$ denotes the half crossing angle (crabbing angle for each beam), ω is the angular frequency of the crab cavity and ϕ_{noise} is the amplitude of the CC phase noise. This equation can be simply derived from the geometrical constraints to provide head-on collisions at the IP and assuming small angles.

The abrupt luminosity loss is caused by an exponential rise of the horizontal emittance for amplitudes above the threshold. Figure 3 shows the simulated time evolution of the electron rms beam size of the for different noise amplitudes. The signature of an instability is clearly observed.

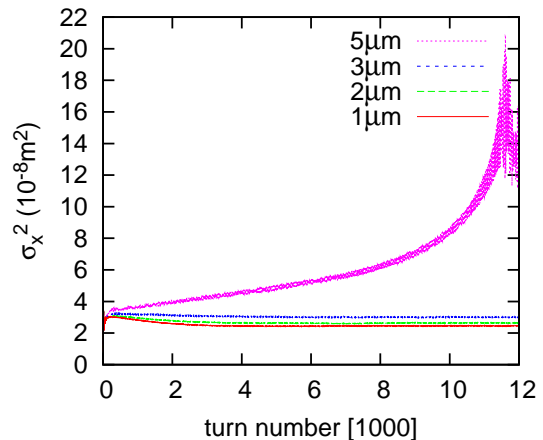


FIG. 3: Simulated rms beam size of the electron beam distribution versus turn number for different noise amplitudes, clearly revealing the existence of a threshold for the onset of the instability.

To understand this unexpected noise-induced instability extensive simulations and analyzes have been performed. The beam-beam interaction characterizes for resulting in two frequency modes (σ - and π -modes) and a continuum spectrum placed in between the modes. The σ -mode features in phase oscillations of the two beams at the IP. On the contrary, the π -mode is characterized for the opposite phase oscillations of the two beam at the IP.

Figure 4 (bottom) shows the simulated relative luminosity versus the frequency of the noise for various noise amplitudes. The top plot illustrates the horizontal spectrum, showing the σ -mode of the beam-beam interaction. This scan reveals that the instability is the strongest at a frequency of 0.523. Exciting closer to the σ -mode at these amplitudes does not cause significant luminosity loss since beams oscillate in phase. Another weaker instability that has a lower amplitude threshold (between $0.3 \mu\text{m}$ and $1 \mu\text{m}$) is observed between 0.55 and 0.56. Some luminosity loss at the largest noise amplitude persists when exciting to the right of the π -mode.

Figure 5 shows the time development of the instability displaying the electron and positron oscillation amplitude and phase difference versus turn number. These have been obtained by performing an FFT every 1000 turns over 1000 turns. The electron and positron beams start oscillating in phase (phase difference is very close to zero at 0 turns) at the driven frequency of 0.523, however a monotonic increase in the phase difference versus time brings the beams to oscillate in opposite phases (π radians) after 9000 turns. The coherent oscillation amplitudes exponentially grow to values larger than the beam size ($\sigma_x \approx 100 \mu\text{m}$ including the beam-beam dynamic focusing). The instability saturates at about 12000 turns as shown in Figs. 3 and 5. The coherent oscillations of the electron and positron beams with exactly opposite phases cause off-centered collisions and, consequently, the

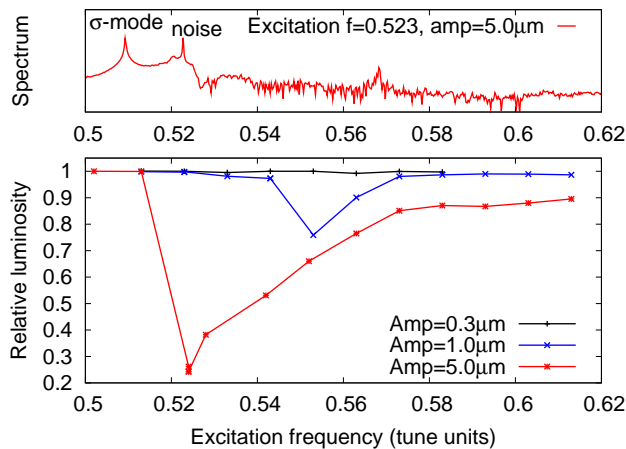


FIG. 4: Bottom: Relative luminosity versus frequency of the noise for three noise amplitudes. Top: Illustration of the horizontal spectrum of the centroid motion for an unstable case, showing the σ -mode and π -mode of the beam-beam interaction.

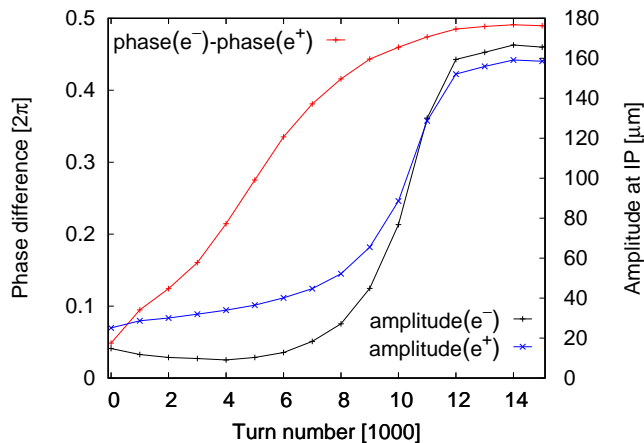


FIG. 5: Time evolution of the driven spectral lines of the horizontal motion of the electron and the positron beams for an unstable case (CC noise at IP is $5 \mu\text{m}$ with frequency 0.523). The phase difference between the driven spectral lines of the two beams is shown versus turn number. The amplitudes of the e^- and e^+ motion at the same frequency are also shown.

luminosity loss. The dephasing of the driven oscillations towards $/\pi$ radians seems to be the key ingredient of the instability since it is not observed in the stable cases. This motivates the following conjecture to explain the instability: Driving large beam oscillations causes a reduction in the π -mode frequency due to the non-linear beam-beam interaction. Therefore when exciting between the σ - and the π -modes there exists an amplitude for which the driving frequency and the π -mode are in resonance.

This conjecture is illustrated by computing the eigenfrequencies of the beam motion in presence of the beam-beam interaction for different oscillation amplitudes. Due to the non-linearity of beam-beam interaction numerical simulations must be performed. The electron and

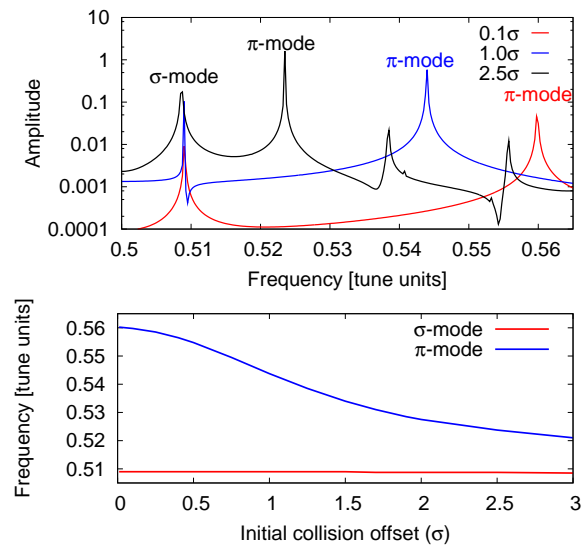


FIG. 6: Illustration of the dependence of beam-beam eigenmodes on the beam oscillation amplitude using a rigid bunch model. Top: horizontal spectrum for three cases with increasing initial collision offset showing a reduction of the π -mode frequency. Bottom: π - and σ -mode frequencies versus initial collision offset.

positron bunches are represented by a single macroparticle to avoid filamentation. The beam-beam kick corresponds to that of a Gaussian bunch with constant beam size. A linear one-turn map is applied to transport the macroparticles of the accelerator. Free oscillation are simulated by giving an initial offset to the macroparticles. Figure 6 shows the results of these simulations. Both top and bottom plots show that for oscillations in the order of 2.5 beam sigma the frequency of the π -mode is reduced to 0.523 as would be required for the resonance condition of Figs. 4 and 5. The consistency between the observations, the multiparticle simulations and the single macroparticle simulations validate, at least to a qualitative level, the previous conjecture for the mechanism of the instability.

Noise driven oscillations are the fundamental reason for the onset of the instabilities. During the 2008 experiments only one of the predicted instabilities was observed (the strong one at frequency of 0.52) and a direct observation of the driven oscillations could not be done for scheduling reasons. Therefore another dedicated experiment in December 2009 was done to search for the weaker instability (at a frequency of about 0.55) and to directly observe the driven oscillations by using the Bunch Oscillations Recorder (BOR) [4]. Figure 7 shows the relative luminosity versus noise frequency as measured during the 2009 experiments, together with model predictions. The measured points at the noise amplitude of $0.4 \mu\text{m}$ clearly reveal the existence of the predicted weaker instability at the frequency of 0.55. The model prediction at $0.4 \mu\text{m}$ shows the loss peak slightly displaced (at 0.56) and with half the amplitude of the measurement. The data for the

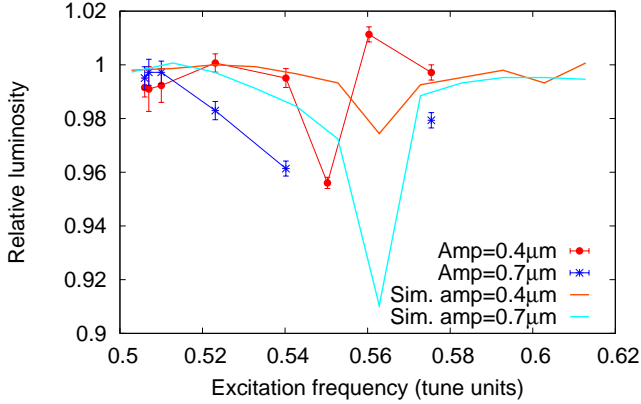


FIG. 7: Relative luminosity versus frequency of the noise for two noise amplitudes, both from measurements and simulations.

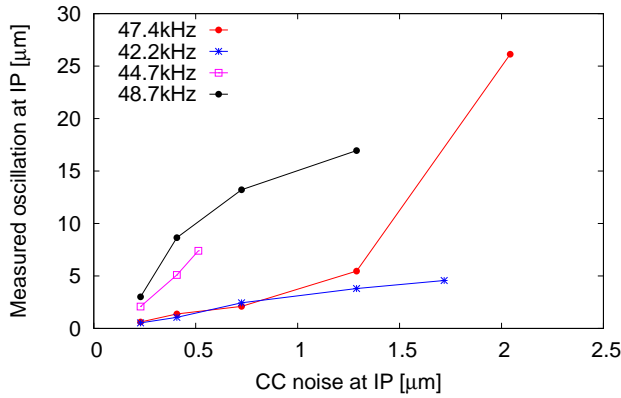


FIG. 8: Observed coherent oscillations versus amplitude of the CC noise excitation. Both quantities expressed as equivalents at the IP location.

amplitude of $0.7 \mu\text{m}$ is not dense enough to locate the loss peak and shows a larger loss than the model prediction at 0.52, 0.54 and 0.58. The small discrepancies between model and measurement at this lower level of losses might be attributed to the uncertainties on beam parameters or to the lack of some ingredient in the simulation. However it is remarkable that the weaker instability was first predicted by simulations and then observed in measurements. Figure 8 shows the measured amplitude of the beam oscillations extrapolated to the IP versus the crab cavity noise amplitude (as expressed in IP equivalent amplitude). The main goal of these data is to confirm the existence of coherent oscillations driven by the CC noise. The order of magnitude of these oscillations is comparable to that predicted by the numerical simulations in Fig. 5.

Amplitude scans were also performed for frequencies close to the vertical tunes, Figs. 9 and 10. The crab cavity deflects in the horizontal plane, therefore in the absence of transverse coupling no resonance effect is expected. Measurement and simulation agree in confirming the ab-

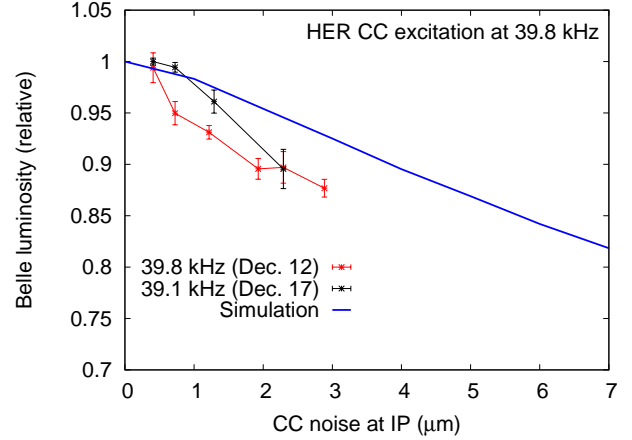


FIG. 9: Luminosity versus HER crab cavity noise as extrapolated to IP displacement. The noise frequency is close to the HER vertical tune.

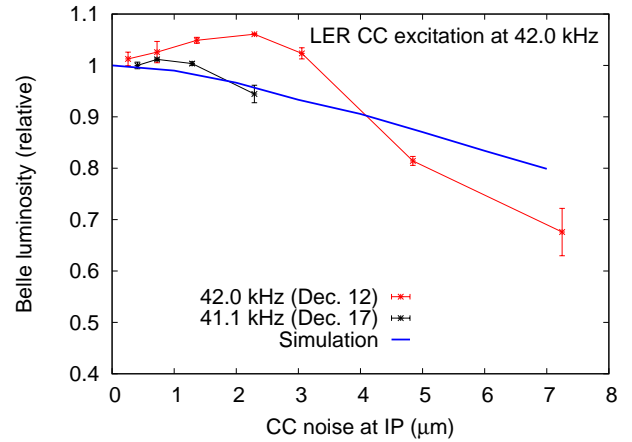


FIG. 10: Luminosity versus LER crab cavity noise as extrapolated to IP displacement. The noise frequency is close to the LER vertical tune.

sence of any instability in the range shown on the plots. However the agreement between measured and simulated luminosity loss is worse than when exciting close to the horizontal tune. This can only be explained by the lack of some ingredient in the simulation like transverse coupling. The LER measurement, in Fig. 10, is the most astonishing showing an increase of the luminosity for the small excitation amplitudes.

III. CRAB DISPERSION

The total deviation of the beam trajectory from the reference orbit can be decomposed as

$$x(s, z) = x_D(s, \delta) + x_\beta(s) + x_{D_{cc}}(z, s), \quad (2)$$

where x_D , x_β and $x_{D_{cc}}$ represent the dispersive, betatron and the crab dispersive orbits, respectively. The z -dependent crab dispersive orbit is given by the following

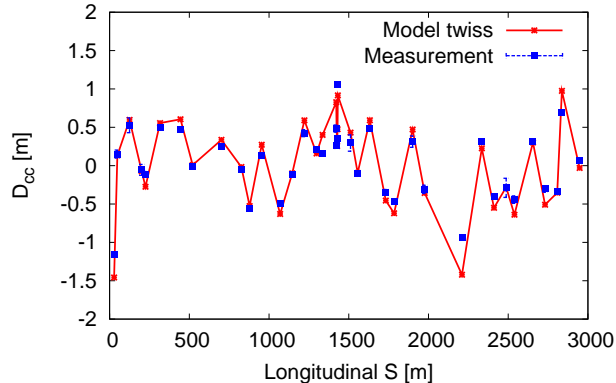


FIG. 11: KEKB Crab cavity dispersion versus longitudinal location both from model (red) and measurement (blue).

equation [7],

$$x_{D_{cc}}(z, s) = \sqrt{\frac{\beta(s)}{\beta^*} \frac{c}{\omega} \tan\left(\frac{\theta}{2}\right)} \frac{\sin\left(\frac{\omega z}{c}\right) \cos(\Delta\varphi_1 - \pi Q)}{\cos(\Delta\varphi_0 - \pi Q)} \quad (3)$$

where $\Delta\varphi_1$ is the phase advance between the crab cavity location and the location s , and $\Delta\varphi_0$ is the phase advance between the crab cavity location and the IP. To have a similar quantity as the off-momentum dispersion, the crab dispersion is defined as:

$$D_{cc}(s) = \frac{x_{D_{cc}}(1\sigma_z, s)}{1\sigma_\delta}. \quad (4)$$

The crab dispersion can be measured in several ways. The simplest one is through orbit differences switching on and off the crab cavity when operating the crab cavity with some phase shift. KEKB regularly operates with a phase shift of 10 degrees. The measured KEKB LER (low energy ring) crab dispersion is compared with the model prediction from Eqs. (2) and (4) and the design TWISS parameters of the KEKB LER. Figure 11 demonstrates that a good agreement is found between the measurement and the model prediction.

IV. CONCLUSIONS

Beam dynamics experiments with crab cavities in KEKB during 2008 and 2009 have served to verify the

theoretical models and to discover noise-driven instabilities in the presence of the beam-beam interaction. These instabilities have been understood as a resonant excitation of the π -mode which exhibits an amplitude dependent frequency. Therefore for certain excitation frequencies there exists an amplitude threshold for which a resonant forced oscillation occurs.

Two instabilities at different frequencies and phase noise amplitudes have been observed both in measurements and simulations. The threshold for the onset of the strongest instability (when frequency is close to the machine tune) is found to be at an IP amplitude of about $4.5 \mu\text{m}$ ($\approx 0.015\sigma_x$ for LER). The weaker instability between 0.55-0.56 (close to the π -mode) develops at $0.4 \mu\text{m}$ ($\approx 0.0013\sigma_x$). This noise amplitude corresponds to 0.02 degrees of the CC phase noise.

The crab dispersion was measured by computing difference orbits switching on and off the crab cavity with 10 degrees phase shift. Model and measurements are in good agreement.

These measurements set the first steps towards the validation of crab cavities in the LHC. On one hand the proton beam in the LHC will not benefit from the cooling by synchrotron radiation but on the other hand the beam-beam tunes of the LHC will not reach the current KEKB beam-beam tunes. Dedicated LHC simulations using the above verified beam dynamics models for CCs should shed light into the phase noise tolerances. Regarding the above results it is advisable to aim at noise levels well below the observed 0.02 degrees for the onset of the weaker instability.

Acknowledgments

R. Miyamoto provided a first version of the rigid bunch tracking code used in this paper. This work is supported by the Large Scale Simulation Program No.09/10-16(FY2009) of High Energy Accelerator Research Organization (KEK). This work is also supported by the European Community-Research Infrastructure Activity under the FP6 "Structuring the European Research Area" programme (CARE, contract number RII3-CT-2003-506395).

-
- [1] S.Kurokawa et al, "KEKB B-Factory Design Report", KEK Report 95-7, August 1995.
 [2] R. Calaga, U. Dorda, R. Tomas, F. Zimmermann, K. Akai, K. Ohmi, K. Oide, "Small angle crab compensation for LHC IR upgrade", Particle Accelerator Conference 2007,

- IEEE.
 [3] K. Ohmi, M. Tawada and Y. Funakoshi, "STUDY OF THE BEAM-BEAM EFFECT FOR CRAB CROSSING IN KEKB AND SUPER KEKB", Proceedings of the Particle Accelerator Conference 2005.

- [4] M. Tobiyama and E. Kikutani, “Development of a high-speed digital signal process system for bunch-by-bunch feedback systems”, *Phys. Rev. ST Accl. Beams* **3**, 012801 (2000)
- [5] M.Arinaga, J.Flanagan, S.Hiramatsu, T.Ieiri, H.Ikeda, H.Ishii, E.Kikutani, T.Mimashi, T.Mitsuhashi, H.Mizuno, K.Mori, M.Teijima and M.Tobiyama, “KEKB Beam Instrumentation Systems”, *Nucl. Instrum. Meth. Phys. Res. A* **499** (2003) 100-137.
- [6] Y. Funakoshi et al., in *Proceedings of European Particle Accelerator Conference 2008*, page 1893 (2008).
- [7] Y. Sun, R. Assmann, J. Barranco, R. Tomás, T. Weiler, F. Zimmermann, R. Calaga, A. Morita, “Beam dynamics aspects of crab cavities in the CERN Large Hadron Collider”, *Phys. Rev. ST-AB* **12**, 101002 (2009).